J Solid State Electrochem
DOI 10.1007/s10008-014-2729-z

ORIGINAL PAPER

Electrochemical nucleation and growth of silicon in the KF-KCl-K_2SiF_6 melt

Yurii P. Zaykov · Sergey I. Zhuk · Andrey V. Isakov · Olga V. Grishenkova · Vladimir A. Isaev

Received: 11 December 2014 / Revised: 29 December 2014 / Accepted: 29 December 2014
© Springer-Verlag Berlin Heidelberg 2015

Abstract The work related to the study of the initial stages of the silicon electrodeposition on the glassy carbon electrode in molten KF-KCl-K_2SiF_6 was performed. The silicon nucleation and growth process was investigated using cyclic voltammetry, chronoamperometry, and scanning electron microscopy. It was shown that the electrocrystallization process occurs by the instantaneous nucleation with diffusion-controlled growth under the studied conditions. The Scharifker-Hills theoretical model was used to calculate the nucleation density and the diffusion coefficient of depositing ions.

Keywords Silicon · Melt · Electrodeposition · Nucleation · Growth · Diffusion

Introduction

Silicon is widely used in electronics, energetics, and many other industrial applications. One of the possible methods of Si obtaining is an electrodeposition from molten salts [1–3]. This approach can be successfully used for the production of silicon which would be applicable for the fabrication of photovoltaic cells, high-efficiency anodes for the lithium-ion chemical power sources, and other devices [4–8]. It is well known that the initial stages of electrodeposition, including nucleation, and growth, in many respects determine the properties and quality of a final deposit. Therefore, a special attention should be paid to studying the nucleation and growth process of new phase on electrode.

As for the silicon electrodeposition from molten salt, the nucleation and growth process has not been thoroughly studied yet. Only a few papers are dedicated to this issue. Carleton et al. [9] have found that the nucleation process is instantaneous and is followed by three-dimensional growth during the Si electrodeposition on the glassy carbon electrode from the KF-LiF-K_2SiF_6 melt at 750 °C. Stern and McCollum [10] considering the Si electrodeposition from the LiF-NaF-KF-K_2SiF_6 melt at 750 °C have concluded that the deposit grows three-dimensionally from simultaneously formed nuclei. Cai et al. [11] studied the Si nucleation process on an electrical steel electrode in the LiF-NaF-KF-Na_2SiF_6 melt at 750 °C. They have determined that the silicon electrocrystallization process was controlled by a progressive three-dimensional mechanism. Bieber et al. [12] have investigated the silicon nucleation and growth process in the molten NaF-KF-Na_2SiF_6 on silver electrode in the temperature range of 820–950 °C and have proved that the Si electrodeposition occurred through the instantaneous nucleation with a diffusion-controlled growth.

The fluoride-chloride molten salts were used as an electrolyte for obtaining Si deposit in works [3, 13, 14]. The main advantage of the fluoride-chloride melts in comparison with the pure fluorides is a possibility to use lower temperatures during electrodeposition; moreover, they are less aggressive.

The purpose of this work was to study the initial stages of the silicon electrodeposition from the KF-KCl-K_2SiF_6 melt. Cyclic voltammetry (CV), chronoamperometry (CA), and scanning electron microscopy (SEM) were used for investigations of kinetics and mechanism of the Si electrodeposition process. The CV showed that the process of the Si electrodeposition occurs by the nucleation and growth mechanism. The chronoamperometric experiments were used for investigating

Y. P. Zaykov · S. I. Zhuk · A. V. Isakov · O. V. Grishenkova · V. A. Isaev (✉)
Ural Branch of the Russian Academy of Sciences, Institute of High Temperature Electrochemistry, 20 Academicheskaya Str., 620990 Ekaterinburg, Russia
e-mail: v.isaev@ihte.uran.ru

Y. P. Zaykov
Ural Federal University, 19 Mira Str., 620002 Ekaterinburg, Russia

Published online: 22 January 2015

the nucleation and growth mechanism of silicon in details. The SEM was applied as an addition to electrochemical methods.

Experimental

The experiments were carried out in a three-electrode hermetic water-cooled stainless steel cell in the atmosphere of high-purity and dehydrated argon. A glassy carbon crucible placed into a Ni-vessel served as a container for the electrolyte. A monocrystalline silicon was used as a reference electrode and as an auxiliary electrode. A working glassy carbon electrode (SU-2000, 99.999 %, UralMetalGraphit) was rinsed with distilled water, ethanol, and dried under vacuum. Typical geometrical surface area of the glassy carbon electrodes varied from 0.6 to 0.8 cm^2.

Chemically pure grade potassium fluoride, chloride, and hexafluorosilicate were used for the electrolyte preparation. This technique is described in details in [15].

The silicon nucleation and growth process was investigated using CV, CA, and SEM analysis. All experiments were carried out in the KCl-KF(1:2)-K_2SiF_6 melt with the silicon concentration of 1.12×10^{-4} mol cm^{-3} (6.77×10^{19} cm^{-3}) at 750 °C. The electrochemical measurements were performed with an Autolab PGStat 302N controlled by a computer supplied with the research software Nova 1.5 and GPES. An electrolyte resistance compensated by Autolab was determined using an impedance method. Before registering each $i(t)$ curve, the anode potential of 1.2 V during 2 s was applied in order to dissolve depositing crystals and to maintain the stable state of the working electrode. The Si crystals were observed by scanning electron microscope Jeol JSM-5900LV.

In this work, the cathode current and overpotential are considered to have positive values.

Results and discussion

Typical cyclic voltammograms for the Si electrodeposition on the glassy carbon electrode in the KF-KCl-K_2SiF_6 melt are shown in Fig. 1. After beginning a scan in the forward direction, the low cathodic current as a result of the double electric layer charging, and the accumulation of single adatoms of new phase on the electrode surface, were observed. After reaching a certain potential, the nucleation and growth process has began that lead to the sharp current increase. Then, the complete layer of the Si deposit forms, and the peak which is observed further is connected with diffusion of ions to a deposit surface (Fig.1a). On the anodic scan, the peak corresponding to the stripping of the earlier deposited silicon is observed.

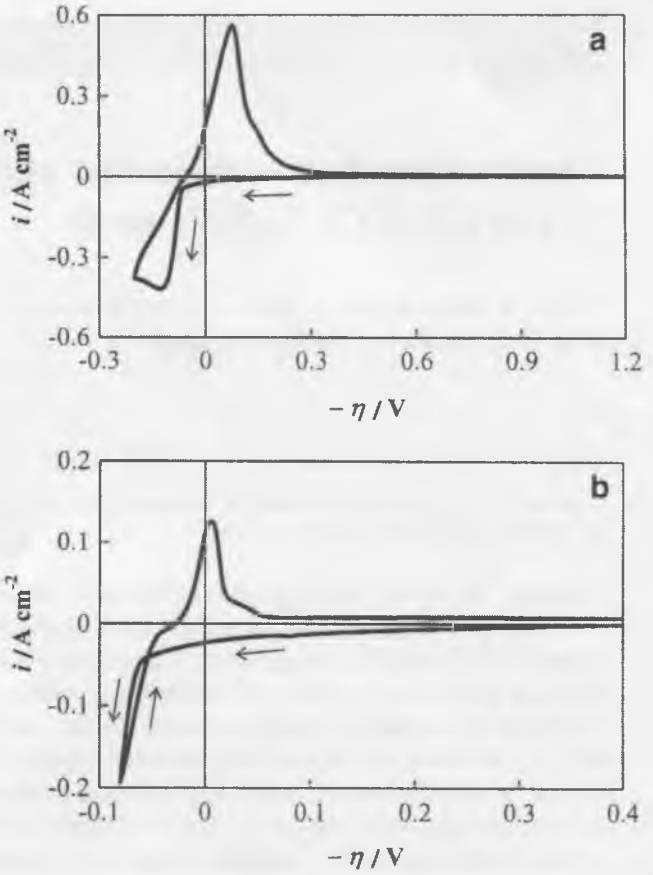

Fig. 1 Cyclic voltammograms for the Si electrodeposition on the glassy carbon electrode at 750°C from KF–KCl–K_2SiF_6 melt; the scan rate is 0.09 V s^{-1} and the reverse potentials are –0.2 V **a**, and –0.08 V **b**. Si monocrystal is the reference electrode

If the reverse of the potential occurs before the formation of the complete silicon layer, then a characteristic hysteresis ("nucleation loop") is appeared and a single anodic peak of the Si stripping takes place (Fig.1b). This is typical for the nucleation and growth mechanism of electrocrystallization [16].

The potentiostatic current density transients $i(t)$ are known to provide the most direct information about the kinetics of electrochemical nucleation and growth. A series of experimental $i(t)$ transients for the Si electrodeposition at different overpotentials are presented in Fig. 2. These transients are typical for the electrocrystallization process occurring by means of three-dimensional nucleation with the diffusion-controlled growth [17–25].

Let us briefly analyze a process of the potentiostatic phase formation in this case. After potential switch, the charge of the double electric layer and the accumulation of adatoms on the electrode take place. After a certain period of time, the nucleation and growth process begins that leads to the current increase. The next stage of the process is characterized by the overlap of the nuclei diffusion zones. The current passes

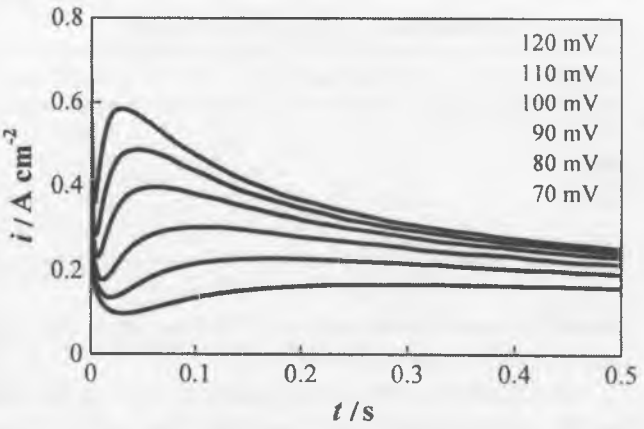

Fig. 2 Typical family of potentiostatic current transients for the Si nucleation and growth on the glassy carbon electrode at different overpotentials

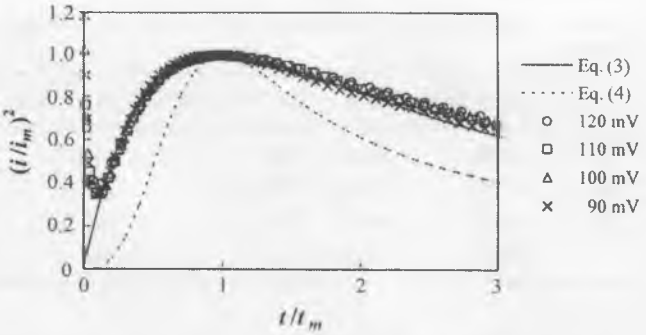

Fig. 3 Comparison of experimental and theoretical dimensionless transients for diffusion-controlled growth: lines correspond to the calculation according to Eq. (3) for instantaneous 3D nucleation, and according to Eq. (4) for progressive 3D nucleation; *symbols* are the experimental date

through the maximum value on this stage. At long times, the planar diffusion to the deposit occurs.

The theoretical treatment of the 3D nucleation process with the diffusion-controlled growth can be found in [17–32]. In our work, the simplest and widely applied Scharifker-Hills theory for the analysis of experimental transients is used. In this theory, for the $i(t)$ transients, the following equations are derived: for the instantaneous nucleation,

$$i = zec(D/\pi t)^{1/2}[1-\exp(-\pi kNDt)], \quad (1)$$

and for progressive nucleation,

$$i = zec(D/\pi t)^{1/2}\left[1-\exp\left(-\pi k' k_0 N_0 D t^2/2\right)\right], \quad (2)$$

where i (A cm^{-2}) is the current density, z is the valency of depositing ions, e (C) is the elementary electric charge, c (cm^{-3}) and D (cm^2 s^{-1}) are the bulk concentration and diffusion coefficient of the depositing ions, respectively, t (s) is the time, $k^2=8\pi c\upsilon$, $k'=4k/3$, υ (cm^3) is the volume of one atom of deposit, $\upsilon=M/\rho N_A$, M (g mol^{-1}) and ρ (g cm^{-3}) are the molar mass and density of the deposit, respectively, N_A (mol^{-1}) is the Avogadro constant, N (cm^{-2}) is the density of nuclei, N_0 (cm^{-2}) is the density of active sites, and k_0 (s^{-1}) is the nucleation rate constant. For the instantaneous nucleation, N is equal to N_0.

Equations (1) and (2) can be expressed in dimensionless form as

$$(i/i_m)^2 = 1.9542\{1-\exp[-1.2564(t/t_m)]\}^2(t/t_m)^{-1}, \quad (3)$$

$$(i/i_m)^2 = 1.2254\left\{1-\exp\left[-2.3367(t/t_m)^2\right]\right\}^2(t/t_m)^{-1}, \quad (4)$$

where i_m and t_m are the maximum coordinates of $i(t)$ transient.

A comparison of the theoretical and experimental dependence $(i/i_m)^2$ vs. (t/t_m) allows determining a mechanism of nucleation. In our case, the experimental curves of the Si electrodeposition and theoretical dependence for the instantaneous nucleation are in a good agreement (Fig. 3). The SEM images of the Si crystals (Fig. 4) obviously confirm the instantaneous character of the nucleation process.

The important relationships [17] allow finding D and N from the transient maximum coordinates

$$i_m^2 t_m = 0.1629(zec)^2 D, \quad (5)$$

$$N = 1.2564/\pi k t_m D. \quad (6)$$

For the small t, from Eq. (1), it follows that

$$i = zeπ\upsilon^{1/2}(2cD)^{3/2}Nt^{1/2}. \quad (7)$$

This equation describes the diffusion-controlled growth of the N isolated nuclei.

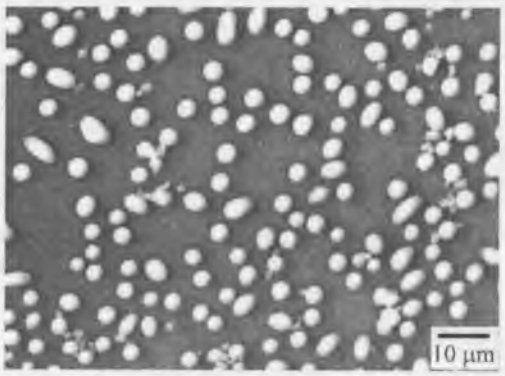

Fig. 4 SEM images of Si crystals on the glassy carbon electrode; η= 80 mV, t=0.18 s

Table 1 Analysis of the current maxima for the Si deposition on glassy carbon

η (mV)	i_m (A cm^{-2})	t_m (s)	$D\times10^5$ (cm^{2}s^{-1})	$N\times10^{-6}$ (cm^{-2})
90	0.303	0.114	3.42	0.556
100	0.396	0.062	3.18	1.10
110	0.484	0.045	3.45	1.40
120	0.583	0.030	3.33	2.17

At long times, Eq. (1) transforms to the Cottrell equation for the planar diffusion

$$i = zec(D/\pi t)^{1/2}. \tag{8}$$

It is clear that the electrodeposition parameters (the diffusion coefficient of the depositing ions and the nucleation density) can be determined by different ways: (1) from analysis of the current maxima, (2) from the initial part of $i(t)$ transients, and (3) from the Cottrell equation.

The characteristics of the current maxima for the potentiostatic Si electrodeposition on the glassy carbon and the calculated values of D and N are given in Table 1. The calculation of D and N was carried out using Eqs. (5) and (6) at z=4 (Si(IV)) and $\upsilon=2.00\times10^{-23}$ cm^3.

Note that the constancy of values $i_m{}^2t_m$ (Eq. 5) also is a validity criterion for the proposed nucleation mechanism. In our case, the value $i_m{}^2t_m$ is equal to 0.0102±0.0005 A^2 s cm^{-4} for the given range of overpotentials.

The initial parts of the experimental potentiostatic $i(t)$ transients are well linearized in the i–$t^{1/2}$ coordinates, that confirms a conclusion about the instantaneous nucleation with the diffusion-controlled growth during the Si electrodeposition (Fig. 5). The diffusion coefficient can be determined according to the Cottrell equation. Using this value D let us find the nuclei density. These values of D and N are presented in Table 2.

As it is seen from Table 1 and 2, the values of D and N determined by the different methods are quite close. Note that

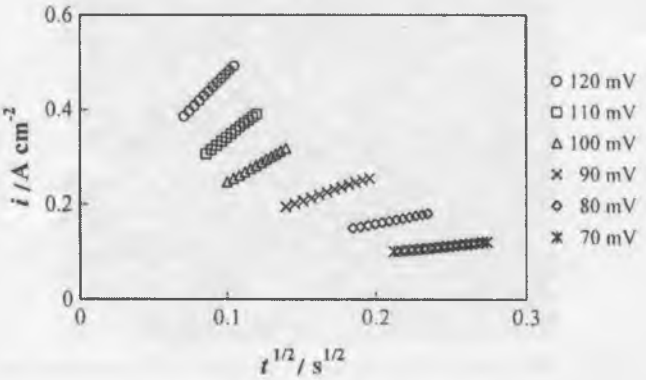

Fig. 5 The initial parts of transients given in Fig. 2 in coordinates i–$t^{1/2}$

Table 2 Calculated values of D (Eq. 8) and N (Eq. 7)

η (mV)	$D\times10^5$ (cm^{2}s^{-1})	$N\times10^{-6}$ (cm^{-2})
90	2.27	0.705
100	2.71	0.923
110	3.09	1.03
120	3.41	1.12

the nuclei density observed in the SEM image (see. Fig. 4) is approximately equal to 2.4×10^6 cm^{-2}.

There is another way for the interpretation of the $i(t)$ transients, which is similar to the one described in [22]. From Eq. (1):

$$-\ln\left(1-ait^{1/2}\right) = \pi kNDt, \tag{9,}$$

where $a=\pi^{1/2}/zecD^{1/2}$

This method allows considering the entire experimental curve and not only the maximum coordinates (i_m, t_m) for calculating N. The same effect can be achieved using Eqs (1), (5), and (6). Then

$$-\ln A = Bt, \tag{10}$$

$$A = 1-0.7154\frac{i}{i_m}\left(\frac{t}{t_m}\right)^{1/2}, \tag{11}$$

$$B = 19.285(i_m/zec)^2t_mkN. \tag{12}$$

The dependences of $-\ln A$ vs. t and the values of N found from the slop of these straight lines are shown in Fig. 6. It is seen that the calculated values of N are close to the values evaluated earlier (Table 1 and 2).

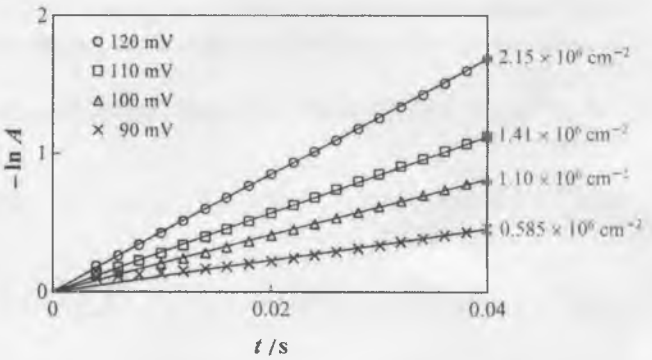

Fig. 6 The dependences $-\ln A$ vs. time calculated from experimental transients using Eqs. (10)–(12). The numbers at the curves denote the nucleation density (N)

Finally, let us note that the galvanostatic conditions for the Si electrodeposition from the KF-KCl-K_2SiF_6 melt were applied in the work [14]. These conditions also can be successfully used for studying the nucleation and growth process [33–36].

Conclusion

The initial stages of the Si electrodeposition on the glassy carbon electrode in the KF-KCl-K_2SiF_6 melt were investigated with the use of electrochemical techniques and SEM. The cyclic voltammetry demonstrated that the Si electrocrystallization process proceeds through the nucleation and growth mechanism. The analysis of chronoamperometric transients established that the initial stage of the Si electrodeposition can be explained on the base of the three-dimensional instantaneous nucleation with the diffusion-controlled growth. The Scharifker-Hills theory was used for experimental results evaluation. The diffusion coefficient of the depositing ions and the nuclei density were calculated using this theory. The SEM method confirmed the results of electrochemical measurements.

Acknowledgments This study was supported by the RFBR, research project No. 13-03-12235 ofi_m.

References

1. Schlesinger TE, Rajeshwar K, De Tacconi NR (2010) Chapter 14 in book modern electroplating, 5th edn. Wiley, New York
2. Elwell D, Rao GM (1988) J Appl Electrochem 18:15–22
3. Frolenko DB, Martem'yanova ZS, Valeev ZI, Baraboshkin AN (1993) Sov Electochem 28:1427–1435
4. Xu J, Haarberg GM (2013) High Temp Mater Process 32:97–105
5. Elwell D, Feigelson RS (1982) Solar Energy Mater 6:123–145
6. Chemezov OV, Isakov AV, Apisarov AP, Brezhestovsky MS, Bushkova OV, Batalov NN, Zaykov YP, Shashkin AP (2013) Electrochem Energetics 13:201–204 (in Russian)
7. Boen R, Bouteillon J (1983) J Appl Electrochem 13:277–288
8. De Lepinay J, Bouteillon J, Traore S, Renaud D, Barbier MJ (1987) J Appl Electrochem 17:294–302
9. Carleton KL, Olson JM, Kibbler A (1983) J Electrochem Soc 130: 782–786
10. Stern KH, McCollum ME (1985) Thin Solid Films 124:129–134
11. Cai Z, Li Y, Tian W (2011) Ionics 17:821–826
12. Bieber AL, Massot L, Gibilaro M, Cassayre L, Taxil P, Chamelot P (2012) Electrochim Acta 62:282–289
13. Frolenko DB, Martem'yanova ZS, Baraboshkin AN, Plaksin SV (1993) Rasplavy (Melts) 5:42–49 (in Russian)
14. Maeda K, Yasuda K, Nohira T, Hagiwara R, Homma T (2014) ECS Trans 64:285–291
15. Zaykov YP, Isakov AV, Zakiryanova ID, Reznitskikh OG, Chemezov OV, Redkin AA (2014) J Phys Chem B 118:1584–1588
16. Fletcher S, Halliday CS, Gates D, Westcott M, Lwin T, Nelson G (1983) J Electroanal Chem 159:267–285
17. Scharifker BR, Hills G (1983) Electrochim Acta 28:879–889
18. Scharifker BR, Mostany J (1984) J Electroanal Chem 177:13–23
19. Sluyters-Rehbach M, Wijenberg JHOJ, Bosco E, Sluyters JH (1987) J Electroanal Chem 236:1–20
20. Mirkin MV, Nilov AP (1990) J Electroanal Chem 283:35–51
21. Isaev VA, Baraboshkin AN (1994) J Electroanal Chem 377:33–37
22. Kelaidopoulou A, Kokkinidis G, Milchev A (1998) J Electroanal Chem 444:195–201
23. Heerman L, Tarallo A (1999) J Electroanal Chem 470:70–76
24. Milchev A, Heerman L (2003) Electrochim Acta 48:2903–2913
25. Hyde ME, Compton RG (2003) J Electroanal Chem 549:1–12
26. Gamburg YD (2003) Russ J Electrochem 39:318–320
27. Gamburg YD (2004) Russ J Electrochem 40:78–85
28. Brylev O, Roue L, Be langer D (2005) J Electroanal Chem 581:22–30
29. Isaev VA (2007) Electrochemical phase formation. UB RAN, Ekaterinburg (in Russian)
30. Branco PD, Mostany J, Borrás C, Scharifker BR (2009) J Solid State Electrochem 13:565–571
31. Díaz-Morales O, Mostany J, Borrás C, Scharifker BR (2013) J Solid State Electrochem 17:345–351
32. Fletcher S (1983) J Chem Soc Faraday Trans 1(79):467–479
33. Milchev A, Montenegro MI (1992) J Electroanal Chem 333: 93–102
34. Hasse U, Fletcher S, Scholz F (2006) J Solid State Electrochem 10: 833–840
35. Isaev VA, Grishenkova OV (2013) J Solid State Electrochem 17: 1505–1508
36. Isaev VA, Grishenkova OV (2014) J Solid State Electrochem 18: 2383–2386